A Review of Methods for Automated Recognition of Casting Defects

Domingo Mery, Thomas Jaeger and Dieter Filbert

May 24, 2002

Abstract

Radioscopy is increasingly being used as a tool for non-destructive testing in industrial production. An example is the serial examination of cast light-alloy workpieces used in the car industry, like aluminum wheels and steering gears. The material defects occurring in the casting process such as cavity, gas, inclusion, and sponge must be detected to satisfy the security requirements; consequently, it is necessary to check 100% of the parts. Since most defects are not visible, X-ray imaging is used for this task. In this paper we present a review of the existing approaches of automated flaw detections in aluminum castings.

Keywords: Automated inspection, flaw detection, image processing, X-ray imaging.

1 Introduction

In the manufacture of die castings, shrinking processes occur during the cooling of the molten metal which can lead to inhomogeneous regions within the workpiece. These are manifested, for example, by bubble-shaped voids or fractures. Voids occur when the liquid metal fails to flow into the die or flows in too slowly, whereas fractures are caused by mechanical stresses when neighboring regions develop different temperature gradients. In addition, other casting defects can occur, such as inclusions or slag formation.

Light alloy castings produced in the automotive industry, such as wheel rims and steering gear boxes are considered to be parts relevant to vehicle safety. In order to insure the safety of their construction, a control of their quality is required.

In the 20^{th} century, radioscopy became the accepted method for the quality control of castings via visual or computer-aided analysis of X-ray images. The purpose of this non-destructive testing method is to locate casting defects which may be located inside the piece and are thus not detectable to the naked eye. An example of one such defective light alloy wheel is shown in the X-ray image in Fig. 1.

Compared to the visual evaluation of X-ray images,

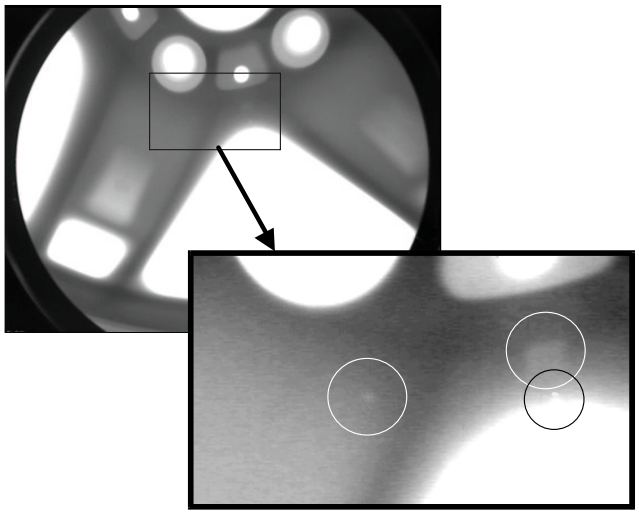

Figure 1: Three voids in an aluminum wheel.

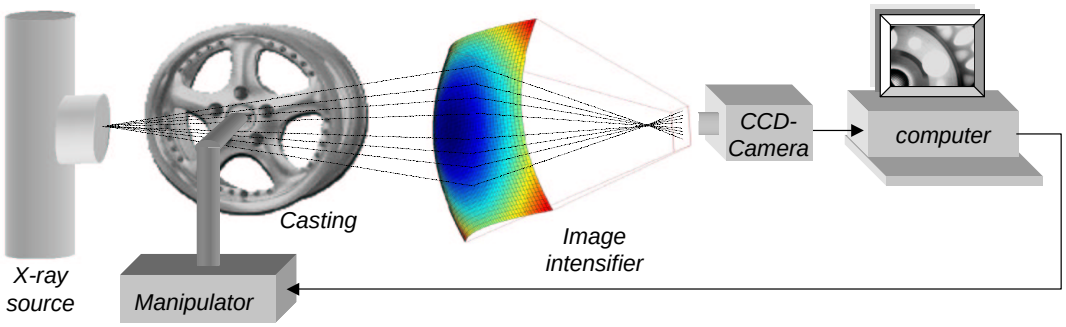

Figure 2: Schematic diagram of an automated X-ray testing stand.

the automatic detection of casting defects offers the advantages of objectivity and reproducibility for all testing results. The essential disadvantages of the proposed methods published to date are their complex configuration and their inflexibility with respect to changes in the piece to be examined (e.g. design modifications), which is not a problem for evaluation by humans.

The principle set up of an automated X-ray inspection unit is shown in Fig. 2. It is typically composed of *i)* a *manipulator* for the handling of the test piece, *ii)* an *X-ray source*, which radiates the test piece with a conical beam and thereby generates an X-ray image of the test piece via central projection, *iii)* an *image intensifier* which transforms the invisible X-ray image into a visible one, *iv)* a *CCD camera* which registers the visible X-ray image and *v)* an *image processor* for the automatic classification of the test piece as satisfactory or defective by digital image processing of the X-ray image and control of the manipulator for positioning the test piece in the desired inspection position[1]. Nowadays, flat detectors made of amorphous silicon are being used as image sensors in some industrial inspection systems [20, 2]. In these detectors, the energy from the X-ray is converted directly into an electrical signal by a semi-conductor (without image intensifier). However NDT using flat detectors is not always feasible because of their high cost compared to image intensifiers.

In this contribution different methods for the automated recognition of casting defects using image processing will be presented. These methods have been described in the literature within the past twenty years and are considered to be the state of the art in this field. One can see that the approaches to detecting can be grouped into three groups: *i)* approaches where a filtering adapted to the structure is performed, which will be described in Section 2; *ii)* approaches using pattern recognition, expert systems, artificial neural networks, general filters or multiple view analyses to make them independent of the position and structure of the test piece, as described in Section 3; *iii)* approaches using computer tomography to make a reconstruction of the cast piece and thereby detect defects, as described in Section 4. Finally, the conclusions drawn in this contribution will be presented in Section 5. A German version of this paper is available in [34].

2 Reference Methods

In reference methods it is necessary to take still images at selected programmed inspection positions. A test image is then compared with the reference image. If a significant difference is identified, the test piece is classified as defective. In order to use a stored refer-

[1]This task is normally performed by a programmable logic controller (PLC).

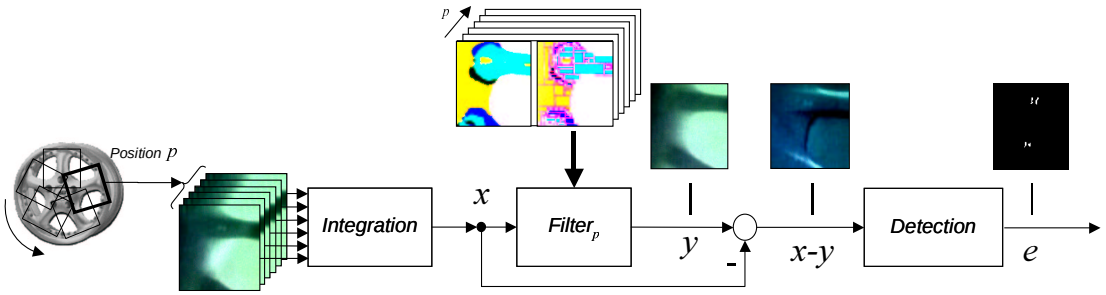

Figure 3: Reference method for automated detection of casting defects.

ence image, the distribution of gray values in the image must correlate to the current image. This makes a very precise positioning of the piece as well as very strict fabrication tolerances and the reproducibility of the X-ray parameters during imaging indispensable. Small variations in these variables lead to great differences between the two images. An alternative approach was suggested by Klatte in the year 1985, whereby the reference image is calculated by filtering directly from the test image [24].

A schematic block diagram for this detection method for the automated recognition of die casting defects is presented in Fig. 3. To reduce the noise level, multiple images taken in a short period of time are averaged (integration) for each programmed position[2]. At first, a defect-free image y is estimated from each integrated X-ray image x using a filter. In this method each test position p has a Filter (Filter_p) which consists of several small masks. The size of these masks and the values for their coefficients should be chosen so that the projected structure of the test piece at position p coincides with the distribution of the masks. After this, an error difference image $x - y$ is calculated. Casting defects are then detected when a sufficiently large difference between X-ray image and reference image occurs. The result of the binary segmentation is shown as e in Fig. 3.

2.1 The MODAN–Filter

The **Mod**ified Medi**an** filter, *MODAN–Filter*, was developed by Heinrich in the 1980's to detect casting defects automatically [9, 17, 18]. With the MODAN–Filter it is possible to differentiate structural contours of the casting piece from casting defects.

The MODAN–Filter is a median filter with adapted filter masks. Note: a median filter is a ranking operator (and thus non-linear) where the output value is the middle value of the input values ordered in a rising sequence [7][3]. If the background captured by the median filter is constant, it is possible that structures in the foreground will be suppressed if the number of values belonging to the structure is less than one half of the input value to the filter. This characteristic is utilized to suppress the defect structures and to preserve the design features of the test piece in the image. An example for the application of a median filter is shown in Fig. 4 including different structures and mask sizes compared to the effects of two linear low-pass filters. One can see that only the median filter completely suppresses the relatively small structures, whereas the relatively large patterns retain their gray values and sharp edges.

The goal of the background image function, thus, is to create a defect-free image from the test image. When calculating the background image function, the MODAN–Filter is used in order to suppress only the casting defect structures in the test image. Locally

[2]To build an arithmetic mean a signal to noise ratio is reached which is proportional to $\sqrt{n}$ with n resulting from the number of images added together.

[3]For an even number of input numbers the median value is the arithmetic mean of the two middle values.

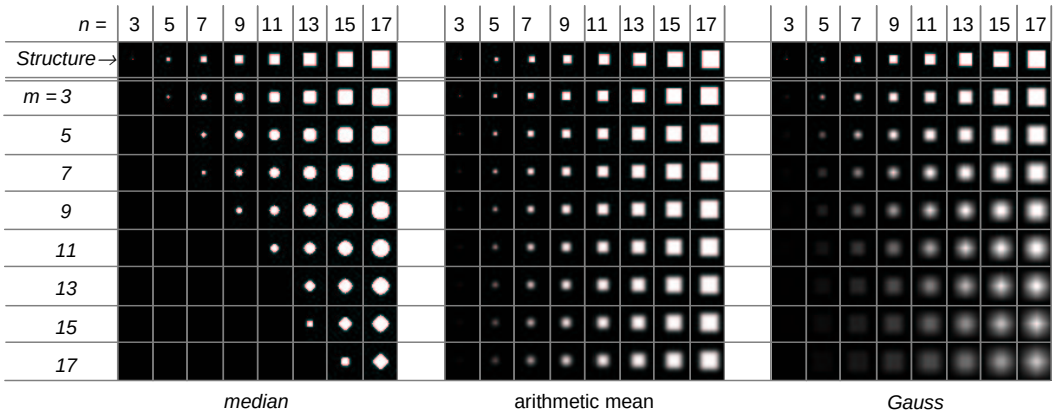

Figure 4: Median filter application on an $n \times n$ structure using an $m \times m$ quadratic mask compared to average and Gauss low-pass filter application.

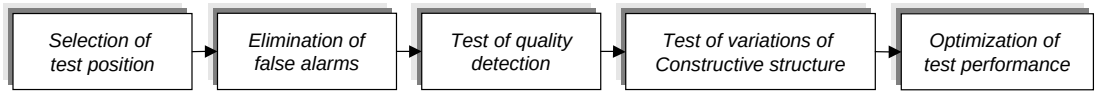

Figure 5: Interactive method for mask selection in a MODAN–Filter.

variable masks are used during MODAN–filtering by adapting the form and size of the median filter masks to the design structure of the test piece. This way, the design structure is maintained in the test image (and the defects are suppressed). Additionally, the number of elements in the operator are reduced in order to optimize the computing time by not assigning all positions in the mask.

Different filter masks are suggested by Heinrich [18]. He has developed automatic and interactive procedures for selecting the MODAN–Filter masks which takes the adaptation to the test piece structure into account. In both procedures the testing positions are chosen manually to ensure that every volume element of the cast piece is inspected. In the automatic procedure the mask is selected for each pixel, which minimizes an objective function for the segment of the test piece. Heinrich suggests the following objective function:

$$Q_{ij}(d,e) = Q^d_{ij}(d,e) + Q^s_{ij}(d,e) + Q^m_{ij}(d,e). \quad (1)$$

The coordinates of the pixel are given by (i,j), and (d,e) represent the height and width of the mask. Q^d, Q^s and Q^m denote the detection defects, spurious reading[4] and the mask matrix size, respectively. The error-free reference image is estimated for the three input values as follows:

$$y[i,j] = \text{median}(x_1, x_2, x_3), \quad (2)$$

with

$$\begin{aligned} x_1 &= x[i,j] \\ x_2 &= x[i+d_{ij}, j+e_{ij}] \\ x_3 &= x[i-d_{ij}, j-e_{ij}], \end{aligned}$$

where $y[i,j]$ are the gray values in the reference image and $x[i,j]$ in the test image at pixel (i,j). The filter

[4]For three input values of the MODAN–Filter (x_1, x_2, x_3) the detection error and spurious reading is defined as $|x_2 - x_1| + |x_2 - x_3|$ and $x_2 - \text{median}(x_1, x_2, x_3)$ respectively [18].

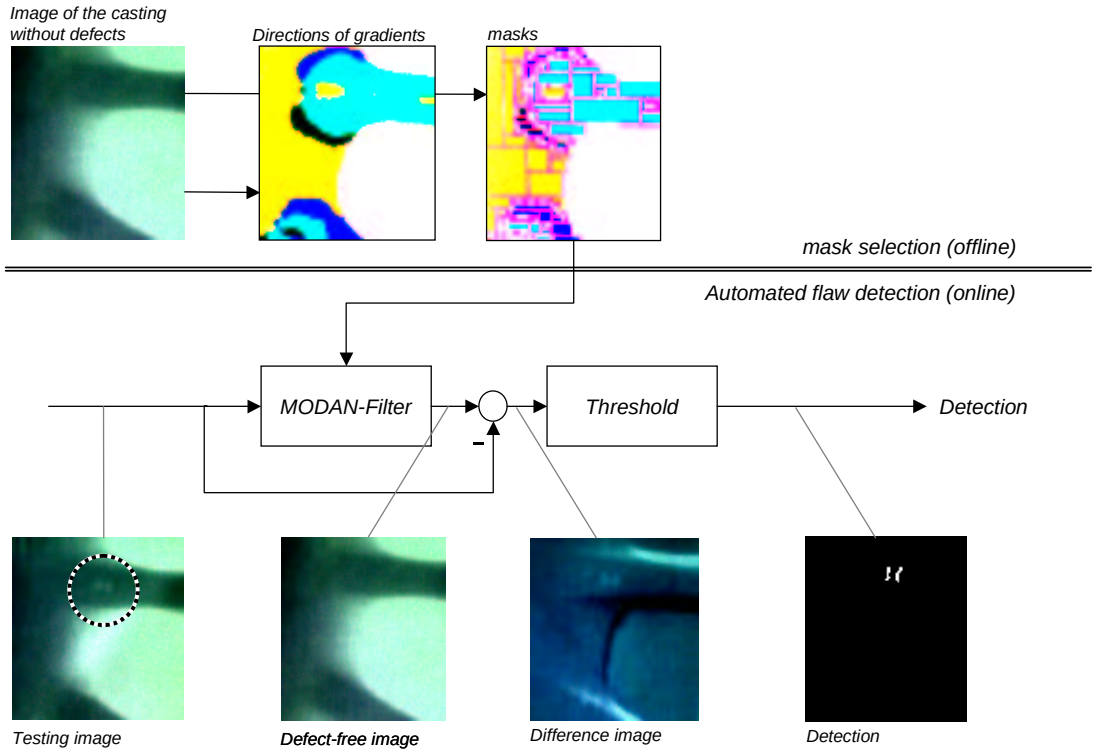

Figure 6: Automatic mask selection for MODAN-Filter and detection after Hecker [16].

direction of the masks is determined by the distances d_{ij} and e_{ij}. Casting defects are detected when

$$|y[i,j] - x[i,j]| > \theta_{ij} \tag{3}$$

This makes it possible to create a good adaptation to the structure of the piece, however, a greater data storage capacity is needed because of the different filter masks used for each pixel. The storage requirements can be reduced in the interactive procedure by choosing the same mask for all rectangular areas in the interactive procedure. This means that

$$\begin{matrix} d_{ij} = d_k \\ e_{ij} = e_k \end{matrix} \quad \text{for} \quad i_k^0 \le i \le i_k^1, \quad j_k^0 \le j \le j_k^1. \tag{4}$$

where i_k^0, i_k^1, j_k^0 and j_k^1 define the boundaries of the k^{th} rectangular mask. The adaptation to the structure is not as exact in this case as in the first procedure.

The interactive procedure is shown in Fig. 5: for every testing position masks with horizontal, vertical and both diagonal filter directions are tested for spurious readings as compared to a defect-free casting. In this step it is decided which direction will not be applied. Next, the objective function (1) is rated in order to select the best mask. The filter masks are to be selected so that variations of the regular structures in the test piece do not lead to spurious readings. Finally, individual filter sectors are combined.

Hecker proposes a method in [16] for the automatic adaptation of the masks to the regular structures of the test piece. For the correct choice of a mask it is necessary to satisfy two criteria: *i)* the corresponding gray values for the structure in the mask must be

constant, and *ii)* the size of the mask must be at least twice as large as in the extent of the casting defect to be found. To fulfill the first criterion, the mask direction is chosen to be perpendicular to the direction of the gradient of the piece's contour. The size of the mask is chosen according to the testing specifications for the extent of the expected casting defect. The method is shown in Fig. 6 (compare with Fig. 3). Only four directions of the gradient are applied: $[0^0 - 180^0]$, $[45^0 - 225^0]$, $[90^0 - 270^0]$ and $[135^0 - 315^0]$, which are shown as four different gray values in Fig. 6. The method generates rectangular regions as appropriate test regions, which have masks with identical directions and sizes.

In [14] Hecker improved the automatic parameterization of the MODAN–Filter. The method which he calls optimized MODAN–Filtering allocates to each pixel the mask from a mask pool which gives the smallest *amplitude error*. For this search, representative piece images are used which were taken of the same piece at the same position. The amplitude error is described by Hecker as the difference between the true expanse of the error depth from the detected value. The pool mentioned above includes 128 different masks with three input values. The masks are distributed among sixteen different mask sizes (16, 17, ..., 31 pixels) along eight different directions ($[0^0 - 180^0]$, $[22,5^0 - 202,5^0]$, ... ,$[157,5^0 - 337,5^0]$).

2.2 Signal Synchronized Filter

Hecker developed the *Signal Synchronized Filter* in [14] to calculate the background image function. This method generalizes the equation used for the MODAN-Filter (2):

$$\begin{aligned} y[i,j] &= \text{median}\{x[i,j], x[i+d_{ij1}, j+e_{ij1}], \\ &\quad ..., x[i+d_{ijn_s}, j+e_{ijn_s}]\}, \end{aligned} \tag{5}$$

where the filter parameters (d_{ijk}, e_{ijk}) are chosen so that the objective function

$$\begin{aligned} &Q_{ijk}(d_{ijk}, e_{ijk}) = \\ &\quad \textstyle\sum_{m=1}^{N_R}\{x_m[i,j] - x_m[i+d_{ijk}, j+e_{ijk}]\}^2 \end{aligned} \tag{6}$$

is minimized when the condition $(d_{ijk}, e_{ijk}) \neq (d_{ijl}, e_{ijl})$ and $d_{ijk}, e_{ijk} > \tau_{min}$ for $k, l = 1, ..., n_s$ with $k \neq l$. The objective function considers N_R representative piece images $\{x_1\}, ..., \{x_{N_R}\}$, which were obtained from the same cast piece and same position. During the experiments only 3 input values ($n_s = 2$) are processed (see Fig. 7). In order to determine the parameters, the number of representative piece images reportedly required is $20 \leq N_R \leq 30$.

Beyond this, Hecker developed the *weighted median operator*, in which the input value $x[i + d_{ijk}, j + e_{ijk}]$ is entered via

$$a_{ijk} \cdot x[i + d_{ijk}, j + e_{ijk}] + b_{ijk}$$

in (5) for $k = 1, ..., n_s$. For the case of the weighted median operator, the objective function is:

$$\begin{aligned} &Q_{ijk}(a_{ijk}, b_{ijk}, d_{ijk}, e_{ijk}) = \\ &\quad \textstyle\sum_{m=1}^{N_R}\{A - a_{ijk} \cdot B + b_{ijk}]\}^2, \end{aligned} \tag{7}$$

with

$$\begin{aligned} A &= x_m[i,j] \\ B &= x_m[i + d_{ijk}, j + e_{ijk}]. \end{aligned}$$

Once (d_{ijk}, e_{ijk}) are identified in (7), one can calculate the coefficients (a_{ijk}, b_{ijk}) to minimize the objective function by linear regression:

$$\begin{aligned} a_{ijk} &= \frac{N_R \sum AB - \sum A \sum B}{N_R \sum B^2 - (\sum B)^2} \\ b_{ijk} &= \frac{\sum A \sum B^2 - \sum AB \sum B}{N_R \sum B^2 - (\sum B)^2} \end{aligned} \tag{8}$$

with summations from $m = 1$ to $m = N_R$. Since the coefficients (a_{ijk}, b_{ijk}) are dependent on d_{ijk} and e_{ijk}, the optimization problem can be formulated, so that the objective function is only a function of the distance parameter (d_{ijk}, e_{ijk}).

As the absolute minimum of the objective function is found by searching, the determination of the filter parameters presents an enormous computational effort. To parameterize the filter at N positions of the test piece, N_R representative piece images per position and $N_I \times N_J$ pixels per image one requires $NN_I^2N_J^2N_R$ comparative operations. When using the weighted median operator, another $8+2N_R$ multiplications and $3+3N_R$ summations must be performed for each comparison to determine the parameters a

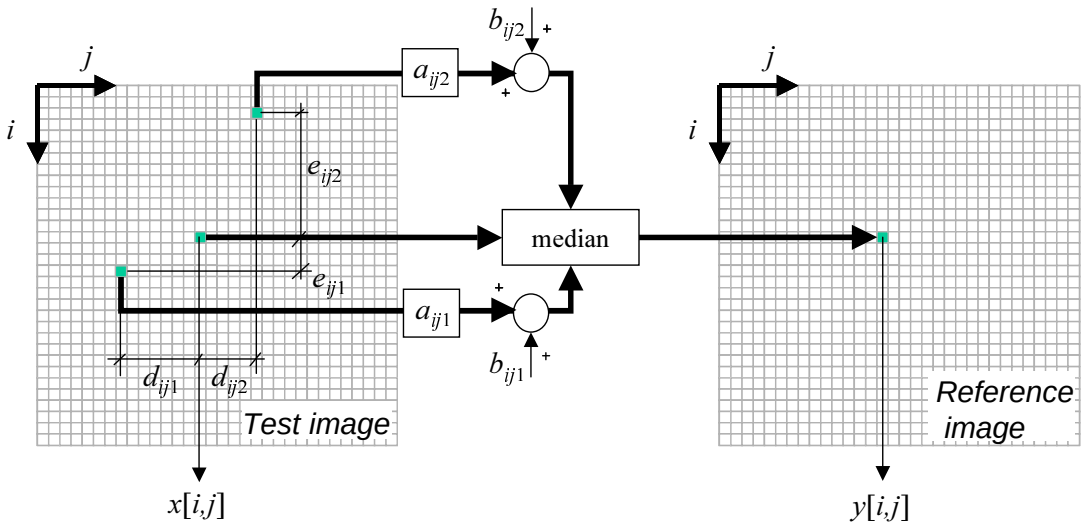

Figure 7: Weighted synchronized filtering (for unweighted filters $a_{ijk} = 1$ und $b_{ijk} = 0$).

and b in (8). Typically, the search for optimal parameters for a test piece takes several weeks. To reduce the computing time Hecker recommends, among other things, that the reference images be subsampled and the reference area be limited where the optimal distance between d and e are sought. Obviously, there must be a compromise between the reduction of computing time and the robustness of the detection. For this reason the reduced computing time required for a robust detection is not yet acceptable for industrial application.

2.3 The PXV 5000 Radioscopic Test System

The radioscopic test system PXV 5000 was developed in the early 1990's by Philips Industrial X-ray GmbH as a fully automatic radioscopic testing device [15, 26]. The system was further developed by YXLON International X-ray GmbH.

The testing system evaluates a random sample of a defect-free test piece in a learning process. Every structure and every irregularity that the system finds in the test piece is classified as a regular structure and entered into an appropriate library [25]. The essential steps in the PXV 5000 system (see block diagram in Fig. 8) are discussed below [33]:

Integration: To suppress the noise level, depending on the application, 4 to 16 X-ray images are integrated at the same test piece position.

Filtering: The PXV 5000 makes the application of up to eight processing steps per position, in which different filters can be selected from a long list of filter algorithms and masks which can be combined freely. In this way, a defect-free X-ray image can be identified in the test image. A difference image is generated from the comparison of both images[5].

Masking: In this step, all irrelevant structures are removed which are located outside of a freely definable mask.

Segmentation: Using a two-threshold procedure, potential defect structures are segmented. The higher threshold value serves to detect the potential defect and the lower to detect the projected size in the image.

[5] A new filtering approach –called AI (Automatic Inspector)– based on neural networks has been recently developed by YXLON [39, 44].

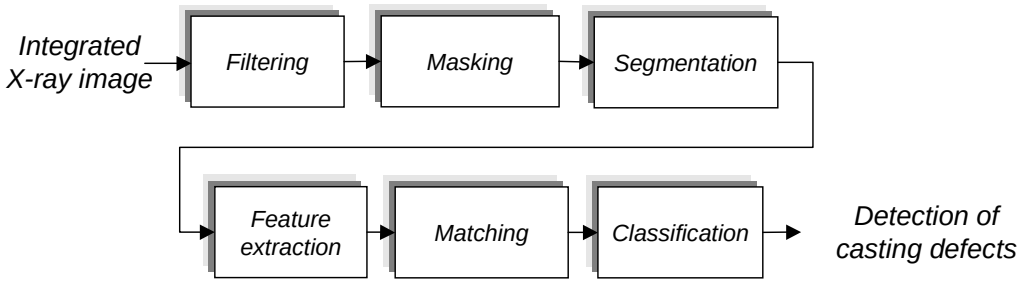

Figure 8: Block diagram of the detection approach used in the PXV 5000.

Feature extraction: Features are extracted (e.g. center, area, perimeter, Feret coordinates[6], measure of compactness, extent, minimum, maximum and average gray level value) from the segments which describe their properties.

Matching and classification: By comparison of the model's features from which they were extracted during the learning process and stored in a library, it is possible to eliminate the regular structures of the piece.

According to YXLON, only 3 defects were detected during the inspection of 600 aluminum die cast pieces. Furthermore, all casting defects larger than 1.56 mm^2 were detected.

2.4 Radioscopic testing system SABA 2000T

The fully automatic radioscopic examination device Seifert Automatic Image Evaluation (SABA) was developed in the late 1980's by the company Rich. Seifert & Co. [38]. Continual improvements in mechanical drives and computer speeds by Seifert made it possible to develop the radioscopic examination device SABA–2000 in the year 1994 [35] and the SABA–2000T in 1998 [36], which reached higher digital image resolutions and faster testing speeds. According to the Seifert company, as reported in [34], the detection approach used in the SABA series has remained unchanged, as it is based on an optimization of the MODAN–Filter (see section 2.1), as developed in the 1980's for the approximation of a defect-free X-ray image. The detection of casting defects is performed as in Fig. 3 . This testing system determined only two deviations during the inspection with 1034 concurring decisions [10, 38].

[6]Coordinates of the lower left corner and upper right corner for the smallest rectangle circumscribing the segment.

3 Methods without a priori knowledge

Methods will be described in this section which can detect casting defects in a test piece without prior knowledge of the piece's structure.

3.1 ISAR Radioscopic testing system

The **I***ntelligent* **S***ystem for* **A***utomated* **R***adioscopic testing* ISAR was developed by the Fraunhofer Institute for Integrated Circuits (IIS-A) in the 1990's [42, 43]. Inspection is performed with the aid of a COMMED filter (*COMbined MEDianfilter*), also developed by the Fraunhofer Institute.

The die cast pieces are identified by the system, so that an examination specifically for that piece can be performed. After the die cast piece is identified, X-ray parameters, testing criteria, translocation of the handling device and inspection positions are selected.

According to IIS-A, the COMMED-Filter can detect casting defects without a priori knowledge of the test piece structure. The algorithm can differentiate between the structure of the test piece (edges, cor-

ners, bore holes etc.) and structures which are not part of the piece. During the testing of wheel rims, for example, the time for image analysis for an aluminum wheel with a diameter of 17" was about 35 s for the required 25 different positions.

3.2 Gayer et al.'s Method

This method for defect detection was originally published in 1990 by Gayer et al. for the testing of welding seams [11]. But the algorithm can also be used for the recognition of casting defects. The proposed method can be summarized as having two steps:
i) A quick search for potential defects in the X-ray image: Assuming that the defects will be smaller than the regular structure of the test piece, potential defects are classified as those regions of the image where higher frequencies are significant. The spectrum of the X-ray image is determined with the help of a fast Fourier transformation, which is calculated either row by row or column by column in little 32×32 windows. When the sum of the higher frequencies of a window is greater than a given threshold value, the entire window is marked as potentially defective. Another possibility is suggested by the authors as part of this task: A window is selected as potentially defective when the sum of the first derivative of the rows and columns of a window is large enough.
ii) Identification and location of the true defect: Because of the time consuming nature of this step, only those regions which were previously classified as being potentially defective are studied here. Two algorithms were developed here as well. The first leads to a matching[7] between the potential defect and typical defects which are stored in a library as templates. Whenever a large resemblance between the potential defect and a template is found, the potential defect is classified as a true defect. The second algorithm estimates a defect-free X-ray image of the test piece by modeling every line of an interpolated spline function without special consideration for the potentially defective region. Following this, the original and the defect-free images are compared. True defects are identified when large difference occur compared to the original input image.

[7] Matching is performed with a *Sequential Similarity Detection method*.

3.3 Kehoe and Parken's Method

In 1992 Kehoe and Parken presented in [23] an intelligent, knowledge-based casting defect detection which utilizes an image processor and an expert system to automatically recognizes die casting defects. The method consists essentially of two steps:
Detection and Analysis: At first, possible defects are segmented in small regions by adaptive thresholding [21]. Then the detected possible defects are fused by dilation and erosion (*closing*) [7]. Finally, geometric characteristics are extracted from the fused regions.
Classification: By using an expert system the regions are segregated into defect classes e.g. bubbles, slack, cracks etc.

This system was tested in the laboratory with eight X-ray images and compared with visual detection. The automated detector was able to identify more defects than human operators could find. The difficulty with this method lies in the creation of a knowledge data bank which includes all possible defects.

3.4 Boerner and Strecker's Method

At the end of the 1980's Boerner and Strecker presented in [3] a method for the automated casting defect recognition which they had developed on their own at the Philips Research Laboratory in Hamburg. As usual, the method is centered on the analysis of individual X-ray images taken at the desired position of the test piece. After improving the image quality with a look-up-table [7] and shading correction [18], the procedure extracts the feature to be segmented in every pixel of the X-ray image.

A classifier is designed to segregate every pixel (i, j) into class k. There are typically only two classes: the class $k = 1$ for a regular structure of the piece and the class $k = 2$ for defects. In general, the method is valid for N_K classes.

With the help of a decision function, the image's pixels are classified. The decision functions are cal-

culated as linear functions with the features

$$d_k[i,j] = a_{k0} + \sum_{p=1}^{n} a_{kp}\ z_p[i,j] \tag{9}$$

or as quadratic functions with the features

$$\begin{aligned} d_k[i,j] \quad = \quad & a_{k0} + \textstyle\sum_{p=1}^{n} a_{kp}\ z_p[i,j] + \\ & \textstyle\sum_{p=1}^{n} \sum_{q=p}^{n} a_{k,p,q}\ z_p[i,j]\ z_q[i,j] \end{aligned} \tag{10}$$

for $k = 1, ..., N_K$. Here $z_p[i,j]$ are the values of the p^{th} extracted feature of the pixel (i,j) for $p = 1, ..., n$ and $a_{k0}, a_{k1}, ...$ are the linear parameters in the decision function. Using a linear regression, these parameters are determined in a learning phase by minimization of the quadratic distance between $d_k[i,j]$ and the idealized decision function $d_k^*[i,j]$. The function $d_k^*[i,j]$ is determined manually out of a random learning sample and assumes the value of 1 or 0 depending on whether the pixel (i,j) belongs to class k or not.

Once the classifier has been learned, a pixel (i,j) in a test image is placed in class k when $d_k[i,j] \geq d_{k'}[i,j] > \theta_k$, for $k' = 1, ..., N_K$ where θ_k is the threshold value for the p^{th} class.

Following this, the defective neighboring pixels are combined to build regions. Finally, a region is detected as being defective if it has a circular form and covers a large enough area.

Boerner and Strecker suggested that the difference between the original image and its image filtered by a DoG[8] or median methods and the rotation invariant *Zernike* feature be named pixel features. The latter designates the use of the gray value of the pixel relative to its surroundings developed in a series of Zernike polynomes [40].

According to the authors, 92% of all defects were recognized with less than 4% false detection in an inspection of 200 die cast pieces. However, the method can only detect circular defects.

[8]The DoG (Difference of Gaussians) filter is calculated as the difference between two Gauss filters. This filtration corresponds to a band pass filter [6, 7].

3.5 Lawson and Parker's Method

In 1994 Lawson and Parker proposed in [27] that artificial neural networks (ANN) can be used for the automated detection of defects in X-ray images. The method generates a binary image from the test image where each pixel is either 0 when a regular structure feature of the piece or 1 when a defect is detected. This entails the supervised learning of a multi-layer perceptron network (MLP) where the attempt is made to obtain a detection from training data. A back propagation algorithm is used for the assignment of weightings within the MLP [4].

The authors use one of two hidden layers in the network topography of the ANN, where the input signal corresponds to a window of $m \times m$ gray values in the X-ray image. The output signal is the pixel at the image center in the binary image. Since the threshold value function for the neurons are sigmoidal in this method, a threshold is used to obtain a binary output signal.

The two hidden layers each have ten cells. During the investigation it was determined that the size of the window for the input signal must be larger than 7×7 ($m > 7$), otherwise, convergence will not be obtained in the learning phase. A group of 50,000 randomly chosen windows were used as the basis of the training data.

The desired detection in the training data was obtained with a segmenting procedure based on an adaptive threshold. During the experiments of five X-ray images, Lawson and Parker show that the detection using ANN is superior to the segmenting method using adapted thresholds. The defects were found successfully and there were no false detections.

3.6 Mery and Filbert's Method

A new method for the automated inspection of aluminum die cast pieces with the aid of monocular X-ray image sequences was presented recently by Mery and Filbert [32, 29]. The procedure is able to perform casting defect recognition in two stages with a single filter and without a priori knowledge of the test piece structure automatically. In the first step, an edge detection procedure based on the Laplacian-of-

Gaussian is employed to find abrupt changes in gray values (edges) in every X-ray image. Here, the zero crossings of the second derivative of the Gauss low-pass filtered image are detected [7]. These edges are then utilized to search for hypothetical flaws defined as regions with a certain area and a high contrast level compared to their surroundings[9].

In the second step, the attempt is made to track the hypothetical casting defects in the sequence of images. False detections can be eliminated successfully in this manner, since they do not appear in the following images and, thus, cannot be tracked. In contrast, the true casting defects in the image sequence can be tracked successfully because they are located in the position dictated by the geometric conditions.

The tracking of the hypothetical casting defects in the image sequence is performed according to the principle of multiple view analysis [31, 13]. Multifocal tensors are applied to reduce the computation time. Following a 3D reconstruction of the position of the hypothetical casting defect tracked in the image sequence, it is possible to eliminate those which do not lie within the boundaries of the test piece.

The elements of this method were tested in a laboratory prototype on simulated [30] and real cases and the preliminary results of detection experiments are promising. In these experiments 24 semi-synthetic and 15 real image sequences were analysed. In the 367 processed images, the existing flaws and more than 12,000 false alarms were flagged in the first step. Nevertheless, the second step was able to recognize 100% of all existing defects with no false detection. Above and beyond this, the required computing time is acceptable for practical applications [41]. As the performance of this method has only been tested on a limited number of image sequences, it will be necessary to analyse a broader databank.

[9]Other methods for segmenting hypothetical casting defects, such as in the PXV 5000 (see Section 2.3) could be used in this first step [33].

4 Industrial Computer Tomography

Another method for the automated detection of casting defects is the (X-ray) computer tomography, which also analyzes the weakening of X-rays as they pass through an object. In contrast to radioscopic testing, two-dimensional computer tomography produces a cross-section of the test piece[10]: two-dimensional images of a flat slice through the investigated object are created out of one-dimensional projections. The projections show the profiles of X-rays weakened by the object, which are measured as a function angularly dependent of the absorption. The emitter must be led around the object in the plane of interest (or the object is rotated) to obtain measurements at different angular positions. This differentiates computer tomography from traditional radioscopic techniques, where the irradiated image is a two-dimensional projection of the object under investigation. The structures contained in the plane of radiation at different depths within the object can be displayed in the cross-sectional image of the computer tomographic reconstruction without overlap (compare Fig. 9).

For the calculation of the object's cross-sectional plane from the measured projections, a great number of algorithms are available which can be classified in general as transformation methods or series development approaches. The methods used in nondestructive materials testing typically belong to the transformation methods. These are based on the projection slice theorem, which states that a one-dimensional Fourier transformation of a projection P_θ at the angle θ is equal to the two-dimensional Fourier transformation of the object function along a straight line through the origin in Fourier coordinates at the angle θ [5, 37] (compare with Fig. 9). The projection P_θ is a function $f(x, y)$ here at the angle θ is designated as the entirety of all line integrals of this angle. A line integral P_θ along a straight line l from A to B is

[10]The word "tomography" is derived from the Greek words $\tau\acute{o}\mu o\varsigma$ and *graphos* and is equivalent to cross-sectional image. The term "computer" corresponds more directly to computation than computer in as such.

defined as

$$p_\theta(r) = \int_l f(x,y)ds, \tag{11}$$

where $f(x,y)$ describes the two dimensional distribution of the X-ray absorption coefficient in the cross-section of the irradiated object, and the straight line l describes the path of a single monoenergetic X-ray beam from the X-ray source through the object to the detector element. The X-ray beam is weakened according to the corresponding law of radiation absorption,

$$I = I_0 \ \exp\left(-\int_l \mu(x,y)ds\right) \tag{12}$$

where $\mu(x,y)$ describes the two-dimensional distribution of the X-ray absorption coefficient which corresponds to the image function $f(x,y)$. In Eq. (12) I_0 stands for the radiation emitted from the X-ray source and I is the radiation incident on the detector after being weakened by the object. After rearranging Eq. (12), the value measured at the detector results:

$$p_\theta = \ln\left(\frac{I_0}{I}\right) = \int_l \mu(x,y)ds \tag{13}$$

A projection P_θ at the angle θ is obtained through realization of a parallel beam geometry, e.g. by shifting the radiation emitter-detector arrangement radially after each measurement. The reconstruction of the object function $f(x,y)$ from its projections presents a typical inverse problem [12].

In practice, however, these ideal conditions cannot be realized [22]. Only a limited number of projection measurements are available for reconstruction, and these are generated from a limited number of line integrals. And thus, a two-dimensional function cannot be uniquely defined. Different image functions can always be created which posses the same projection.

For three-dimensional computer tomography, methods are used which analyze two-dimensional projections[11]. Feldkamp describes a mathematical method in [8] for the calculation of three-dimensional

[11]The problems founded in the principle of tomography persist: three-dimensional results also exhibit a dimension one higher than the projections which are analyzed (two-dimensional 'images').

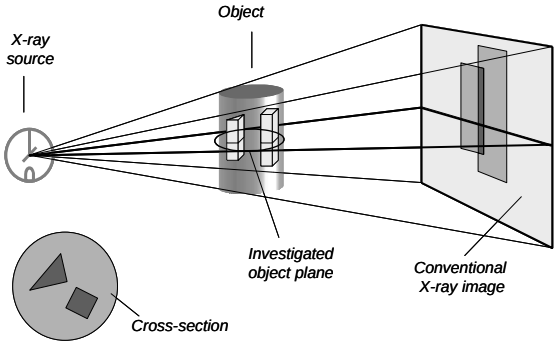

Figure 9: Comparison between a conventional X-ray image and the result of a computer tomographic reconstruction.

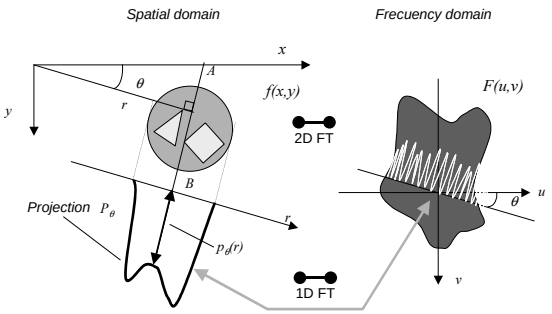

Figure 10: Projection slice theorem.

results with a *cone beam* projection. Other methods adhere to another approach, whereby the results of conventional 2D tomography are layered on top of each other according to their respective positions in the object and the values between the individual (reconstructed) object planes are interpolated.

Common to all of the methods using transformation is the use of filters with low-pass characteristics. This has a negative impact especially on the use in casting piece inspection, since great discontinuities in the measured values result from the object edges in the projections (highly absorptive material next to hollow spaces in the design). The leads to large artifacts, which can make image analysis impossible. In order to obtain high local resolution in the reconstructed object, it is desirable that the X-

ray tube have as small a focal point as possible. In microfocus computer tomography (μCT) resolutions on the order of a few μm are obtainable. To penetrate the aluminum die cast pieces with relevant material thickness for use in the automotive industry, a minimum energy level is needed which lies above the specifications of most microfocal tubes. The problem posed lies in the heat removal, which must occur rapidly enough that any possible damage to the tube is prevented.

Furthermore, computer tomography is a very time intensive process requiring a minimum measurement time for adequate signal to noise ratios as well as a minimum number of projections for the desired local resolution. As a result of the physical reasons which dictate that a minimum measurement time be given for each angular position, the only remaining way to reduce the measurement time is to reduce the number of measurement positions. In those cases where measurement data are lacking, one speaks of a 'limited data problem' [19]. Apart from the reduced measurement time, it can be desirable in industrial applications to analyze only selected projections for reconstruction. Reasons for these selections may lie both in the difficulty in obtaining data for certain angular positions or regions and in the projections of certain objects which are unsuitable for analysis (e.g. polyvalent X-ray absorption properties, inadequate signal to noise ratio for all angular positions).

No industrial applications are known to the authors for this area of 'limited data problems'. Research work is underway with different approaches to optimizing the computations as well as modifications to known algorithms.

5 Conclusions

In this article the fundamental principles of various methods for the automated detection of die casting defects have been explained. These methods have appeared in the literature in the past twenty years and show the development of this sector in the areas of industry and academia.

The detection approaches were divided roughly into three groups: reference methods, methods without a priori knowledge and computer tomography.

As a result of its peak detection performance, the methods of the first group have become most widely established in industrial applications. These methods suffer from the complicated configuration of their filtering, which is tailored to the test piece. Typically, this optimization process takes two or more weeks, independently of whether it is performed manually or automatically.

The prerequisite for the use of a method from the second group is the existence of common properties which define all casting defects well and also differentiate them from design features of the test pieces. These prerequisites are often fulfilled only in special testing situations.

The industrial use of computer tomography for the inspection of die cast parts for the automotive industry is currently limited to the areas of materials research and development as well as to the inspection of especially important and expensive parts [1, 28]. The reasons for this lie both in the great time requirements for measurements and in the insufficient local resolution in economically priced systems, when small defects are to be detected.

Acknowledgments

The authors wish to thank the German Academic Exchange Service, DAAD, the Technische Universität Berlin, the Universidad de Santiago de Chile, and the company YXLON International X-ray GmbH from Hamburg, Germany for the support of this research.

References

[1] I. Bauscher and U. Hassler. Fortschritte in der Computertomographie. In *Berichtsband der Jahrestagung der Deutschen, Österreichischen und Schweizerischen Gesellschaft für Zerstörungsfreie Prüfung (DACH)*, Innsbruck, Austria, 29.-31. Mai 2000.

[2] K. Bavendiek, A. Krause, and A. Beyer. Durchsatzerhöhung in der industriellen Röntgenprüfung – Eine Kombination aus innovativem Prüfablauf und optimierter Bildauswertung. In *DGZfP Jahrestagung*, volume Berichtsband 63.1, pages 301–306, Bamberg, 7-9 Sept. 1998. Deutsche Gesellschaft für Zerstörungsfreie Prüfung e.V.

[3] H. Boerner and H. Strecker. Automated x-ray inspection of aluminum casting. *IEEE Trans. Pattern Analysis and Machine Intelligence*, 10(1):79–91, 1988.

[4] H.-H. Bothe. *Neuro-Fuzzy-Methoden: Einführung in Theorie und Anwendungen*. Springer, Berlin, Heidelberg, 1998.

[5] R.N. Bracewell. Strip integration in radio astronomy. *Astrophysical Journal of Physic*, (9):198–217, 1956.

[6] J. Canny. A computational approach to edge detection. *IEEE Trans. Pattern Analysis and Machine Intelligence*, PAMI-8(6):679–698, 1986.

[7] K.R. Castleman. *Digital Image Processing*. Prentice-Hall, Englewood Cliffs, New Jersey, 1996.

[8] L.A. Feldkamp, L.C. Davis, and J.W. Kress. Practical cone-beam algorithm. *Journal of the Optical Society of America A-Optics Image Science and Vision*, 1(6):612–619, 1984.

[9] D. Filbert, R. Klatte, W. Heinrich, and M. Purschke. Computer aided inspection of castings. In *IEEE-IAS Annual Meeting*, pages 1087–1095, Atlanta, USA, 1987.

[10] Deutsche Gessellschaft für Zerstörungsfreie Prüfung e.V. *Radioskopie, Unterlagen für den Grundkurs Stufe 2*. Deutsche Gesellschaft für Zerstörungsfreie Prüfung e.V., 1996. RS2 2.96.

[11] A. Gayer, A. Saya, and A. Shiloh. Automatic recognition of welding defects in real-time radiography. *NDT International*, 23(4):131–136, 1990.

[12] C.W. Groetsch. *Inverse Problems in the Mathematical Sciences*. Vieweg, Braunschweig, Wiesbaden, 1993.

[13] R. Hartley. Lines and points in three views and the trifocal tensor. *International Journal of Computer Vision*, 22(2):125–150, 1997.

[14] H. Hecker. *Ein neues Verfahren zur robusten Röntgenbildauswertung in der automatischen Gußteilprüfung*. PhD thesis, vom Fachbereich Elektrotechnik, Technische Universität Berlin, 1995.

[15] H. Hecker. PXV 5000.2, Vollautomatische Röntgenprüfung, Bedienungsanleitung. Technischer Bericht, Philips Industrial X-Ray GmbH, Hamburg, 1996.

[16] H. Hecker and D. Filbert. Röntgendurchleuchtungsprüfung: Automatische Anpassung eines Prüfsystems an Prüfaufgaben. In *DGZfP Jahrestagung*, volume Berichtsband 33.2, pages 655–660, Fulda, 27.-29. April 1992. Deutsche Gesellschaft für Zerstörungsfreie Prüfung e.V.

[17] W. Heinrich. Ein zeitoptimaler Rangordnungsoperator für die Automatisierung der radiologischen Gußteilprüfung. Technischer Bericht 123, Institut für Allgemeine Elektrotechnik, Technische Universität Berlin, 1987.

[18] W. Heinrich. *Automatische Röntgenserienprüfung von Gußteilen*. PhD thesis, Institut für Allgemeine Elektrotechnik, Technische Universität Berlin, 1988.

[19] Th. Jaeger. *Optimierungsansätze zur Lösung des* limited data problem *in der Computertomographie*. Verlag Dr. Köster, Berlin, 1997.

[20] Th. Jaeger, U. Heike, and K. Bavendiek. Experiences with an amorphous silicon array detector in an ADR application. In *International Computerized Tomography for Industrial Applications and Image Processing in Radiology, DGZfP Proceedings BB 67-CD*, pages 111–114, Berlin, March 15-17 1999. Deutsche Gesellschaft für Zerstörungsfreie Prüfung e.V.

[21] B. Jähne. *Digital Image Processing*. Springer, Berlin, Heidelberg, 4 edition, 1997.

[22] A.C. Kak and M. Slaney. *Principles of computerized tomographic imaging*. IEEE, New York, 1988.

[23] A. Kehoe and G.A. Parker. An intelligent knowledge based approach for the automated radiographic inspection of castings. *NDT & E International*, 25(1):23–36, 1992.

[24] R. Klatte. *Computergestützte Röntgenprüfung zur objektiven Qualitätssicherung von Werkstücken*. PhD thesis, Institut für Allgemeine Elektrotechnik, Technische Universität Berlin, 1985.

[25] J.-M. Kosanetzky. Optimierung des Produktionsprozesses in der Gießerei-Industrie durch vollautomatische Röntgenprüfung. In *DGZfP Jahrestagung*, volume Band 59.2, Dresden, 1997. Deutsche Gesellschaft für Zerstörungsfreie Prüfung e.V.

[26] J.-M. Kosanetzky and H. Putzbach. Modern x-ray inspection in the automotive industry. In *Proceedings 14th World Conference of NDT (14^{th}–WCNDT)*, New Delhi, Dec. 8-13 1996.

[27] S.W. Lawson and G.A. Parker. Intelligent segmentation of industrial radiographic images using neural networks. In *Machine Vision Applications and Systems Integration III, Proc. of SPIE*, volume 2347, pages 245–255, November 1994.

[28] M. Maisl, H. Reiter M. Purschke, E. Zabler, and M. Rosenberger. Industrielle 3D-Computertomographie. In *Berichtsband der Jahrestagung der Deutschen, Österreichischen und Schweizerischen Gesellschaft für Zerstörungsfreie Prüfung (DACH)*, Innsbruck, Austria, 29.-31. Mai 2000.

[29] D. Mery. *Automated Flaw Detection in Castings from Digital Radioscopic Image Sequences*. Verlag Dr. Köster, Berlin, 2001. (Ph.D. Thesis in German).

[30] D. Mery. Flaw simulation in castings inspection by radioscopy. *INSIGHT, Journal of the British Institute of Non-Destructive Testing*, 43(10):664–668, 2001.

[31] D. Mery and D. Filbert. Die Epipolargeometrie in der Röntgendurchleuchtungsprüfung: Grundlagen und Anwendung. *at - Automatisierungstechnik*, 48(12):588–596, 2000.

[32] D. Mery and D. Filbert. Verfolgung von Gußfehlern in einer digitalen Röntgenbildsequenz – Eine neue Methode zur Automatisierung der Qualitätskontrolle von Gußteilen. *tm - Technisches Messen*, 67(4):160–165, 2000.

[33] D. Mery, D. Filbert, and N. Parspour. Improvement in automated aluminum casting inspection by finding correspondence of potential flaws in multiple radioscopic images. In *Proceedings of the 15th World Conference on NDT (*15^{th}*–WCNDT)*, Rome, Oct. 15-21 2000.

[34] D. Mery, Th. Jaeger, and D. Filbert. Automatische Gussfehlererkennung: Stand der Technik. *tm - Technisches Messen*, 68(7-8), 2001.

[35] M. Purschke and H. Schulenburg. Neue Möglichkeiten der objektiven Durchleuchtungsprüfung. In *DGZfP Jahrestagung*, pages 145–151, Timmendorfer Strand, 9-11 Mai 1994. Deutsche Gesellschaft für Zerstörungsfreie Prüfung e.V.

[36] M. Purschke and H. Schulenburg. Fortschritte der vollautomatischen Röntgenprüfung. In *DGZfP Jahrestagung*, volume Berichtsband 63.1, pages 309–317, Bamberg, 7-9 Sept. 1998. Deutsche Gesellschaft für Zerstörungsfreie Prüfung e.V.

[37] J. Radon. Über die Bestimmung von Funktionen durch ihre Integrale längs gewisser Mannigfaltigkeiten. *Ber. Sächs. Akad. Wiss.*, Math. Phys. Kl.(69):262–277, 1917.

[38] M. Schaefer and M. Purschke. Vollautomatische Röntgenprüfung - zuverlässig und wirtschaftlich. *Sonderausdruck der Zeitschrift 'Qualität und Zuverlässigkeit'*, 36(7), 1991. München.

[39] G. Theis and T. Kahrs. Vollautomatische Inline-Röntgenprüfung von Aluminumrädern. In *DGZfP Jahrestagung*, Berlin, 21.-23. Mai 2001. Deutsche Gesellschaft für Zerstörungsfreie Prüfung e.V.

[40] A. Wallin and O. Kübler. Complete sets of complex Zernike moment invariants and the role of the pseudoinvariants. *IEEE Trans. Pattern Analysis and Machine Intelligence*, 17(11):1106–1110, 1995.

[41] I. Weiske, D. Mery, C. Geisert, and D. Filbert. Implementation of a method for flaw detection in aluminium castings. *e-Journal on Non-destructive Testing*, 7(3):March, 2002.

[42] T. Wenzel. *ISAR: Ein intelligentes System zur automatischen Röntgenprüfung*. Fraunhofer-Institut für Integrierte Schaltungen, Erlangen, 1996.

[43] T. Wenzel and R. Hanke. Fast image processing on die castings. In *Anglo-German Conference on NDT Imaging and Signal Processing*, Oxford, 27-28 March 1998.

[44] YXLON. The new image of automatic defect recognition. *Technical Articles of YXLON International*, 2002. `http://www.yxlon.com/technical_articles.htm`.